Supporting Information

Revealing the Electronic Structure of Organic Emitting Semiconductors at Single-Molecule level

Mingzhu Huang, Jianqiao Dong, Zhiye Wang, Yunchuan Li, Lei Yu, Yichong Liu, Gongming Qian and Shuai Chang

The State Key Laboratory of Refractories and Metallurgy, and Institute of Advanced Materials and Nanotechnology, Wuhan University of Science and Technology, Wuhan 430081, China;

S1. General information

S2. Single molecular conductance measurement with Au electrodes

S3 Conductance measurements with Pt electrodes

S4. 2D Conductance displacement histogram with Au electrodes

S5. Current-voltage measurements with Au electrodes

S6. Electronic structure and Transport calculations

S1. General information

^{1}H NMR & ^{13}C NMR spectra were acquired on a Bruker NMR spectrometer operating at 600 and 150 MHz, respectively, with samples dissolved in CDCl$_3$. UV-vis absorption and photoluminescence spectrum measured on a Shimadzu UV-2000 and Shimadzu RF-5301PC spectrophotometers. Cyclic voltammetry (CV) was performed on a CHI600D electrochemical workstation in dichloromethane (DCM) of 0.1 mol L^{-1} tetrabutylammoniumhexafluorophosphate (TBAPF) as supporting electrolyte under Nitrogen atmosphere. A glassy carbon working electrode and a Pt wire counter electrode against a Ag/AgCl reference electrode (in saturated KNO$_3$) was adopt as the three electrode system. Materials, including solvents and chemicals were used without further purification after purchasing from commercial suppliers.
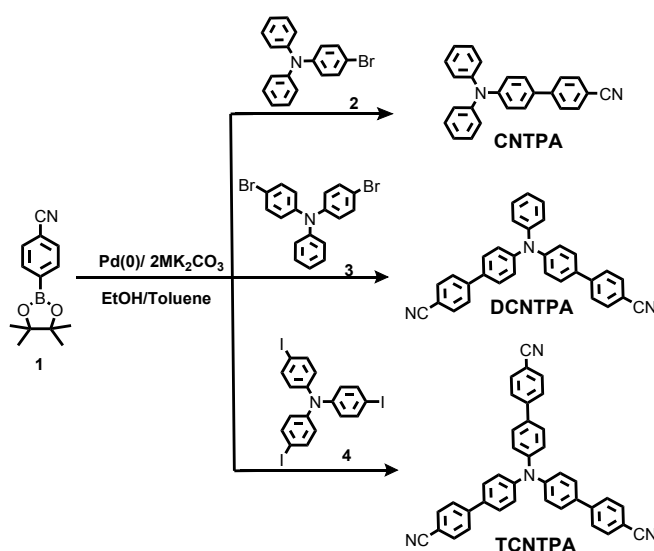
Scheme 1 The synthesis routine of CN-TPA, DCN-TPA, and TCN-TPA.

4'-(diphenylamino)-[1, 1'-biphenyl]-4-carbonitrile (CN-TPA)

Toluene (60 mL), ethanol (20 mL), 2 M aqueous Na$_2$CO$_3$ (15 mL) and a mixture of 1 (0.252 g, 1.1 mmol), 2 (0.324 g, 1.0 mmol) were added into three necks flask, the reaction mixture was bubbled for 15 minutes before adding Pd(PPh$_3$)$_4$ (52 mg, 3 mol %). The reaction was bubbled for another 15 minutes, and then the suspension was stirred at 90 °C overnight under a nitrogen atmosphere. When cooled to room temperature, the mixture was extracted with CH$_2$Cl$_2$ and dried over MgSO$_4$. After the

removal of solvent, the residue was purified by column chromatography on silica gel to afford **CN-TPA** (0.16 g, yield 47%) as a white solid. ^{1}H NMR (600 MHz, Chloroform-d) δ 7.71 – 7.68 (m, 1H), 7.65 (d, J = 8.5 Hz, 1H), 7.49 – 7.44 (m, 1H), 7.32 – 7.27 (m, 1H), 7.16 – 7.12 (m, 2H), 7.08 (t, J = 7.4 Hz, 1H). ^{13}C NMR (151 MHz, cdcl₃) δ 148.54 (s, 2H), 147.23 (s, 3H), 145.03 (s, 2H), 132.55 (s, 9H), 132.11 (s, 2H), 129.39 (s, 19H), 127.83 (s, 10H), 126.90 (s, 8H), 124.91 (s, 20H), 123.54 (s, 10H), 122.98 (s, 11H), 119.09 (s, 1H), 110.04 (s, 1H). MS (MALDI-TOF): m/z calcd for $C_{25}H_{18}N_2$ 346.15; found 346.163.
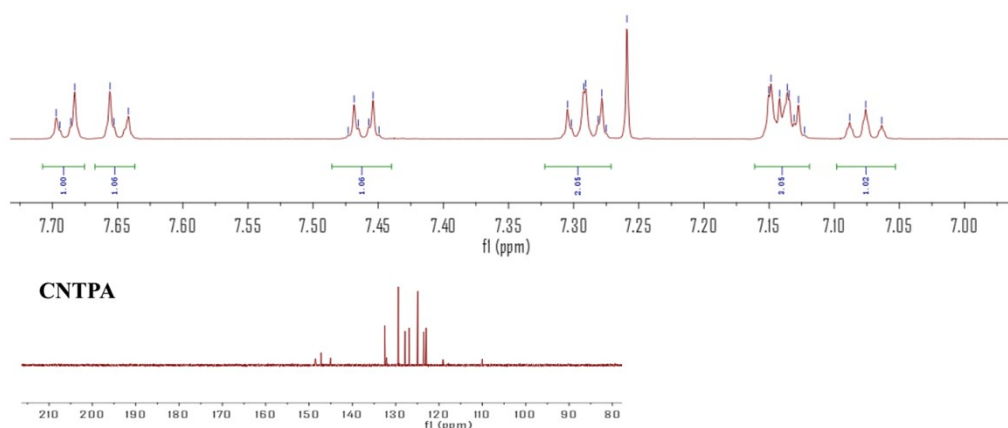
4', 4'''-(phenylazanediyl)bis(([1, 1'-biphenyl]-4-carbonitrile)) (DCN-TPA)

DCN-TPA (0.23 g, yield 51%) was synthesized as a yellow solid in a similar procedure of CN-TPA with 3 instead of 2. ^{1}H NMR (600 MHz, Chloroform-d) δ 7.75 – 7.63 (m, 8H), 7.55 – 7.47 (m, 4H), 7.36 – 7.31 (m, 2H), 7.23 – 7.17 (m, 6H), 7.14 (tt, J = 7.1, 1.2 Hz, 1H). ^{13}C NMR (151 MHz, Chloroform-d) δ 147.13, 138.95, 136.94, 136.48, 127.76, 127.74, 127.44, 124.25, 123.42, 76.94, 31.59, 30.26, 28.92, 22.61, 14.12. MS (MALDI-TOF): m/z calcd for $C_{32}H_{21}N_3$ 447.17; found 447.175.
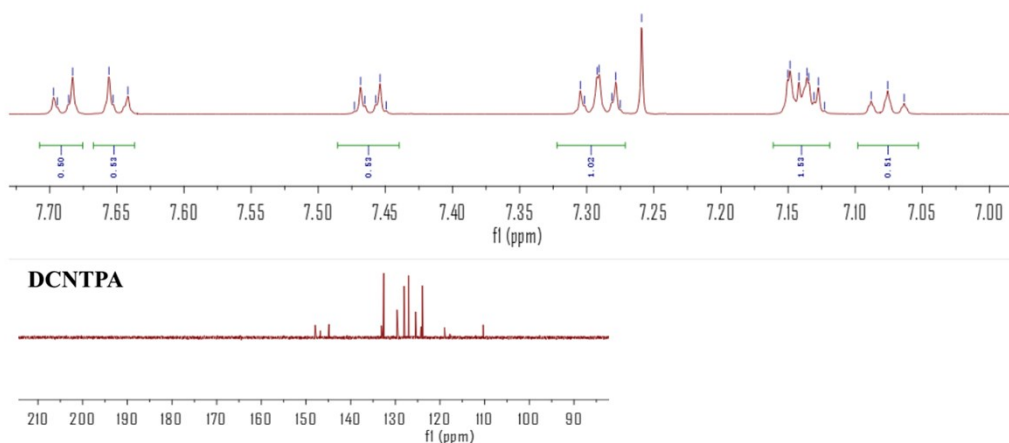
4',4''',4'''''-nitrilotris(([1,1'-biphenyl]-4-carbonitrile)) (TCN-TPA)

TCN-TPA (0.41 g, yield 76%) was synthesized as a yellow solid in a similar procedure of CN-TPA with 4 instead of 2. ^{1}H NMR (600 MHz, dmso) δ 7.87 (q, J = 8.3 Hz, 2H), 7.75 (d, J = 8.4 Hz, 1H), 7.19 (d, J = 8.4 Hz, 1H).^{13}C NMR (151 MHz, dmso) δ 147.45 (s, 1H), 144.25 (s, 1H), 133.35 (d, J = 19.1 Hz, 6H), 128.84 (s, 4H), 127.43 (s, 5H), 124.84 (s, 4H), 109.96 (s, 1H). MS (MALDI-TOF): m/z calcd for $C_{39}H_{24}N_4$ 548.20; found 548.215.
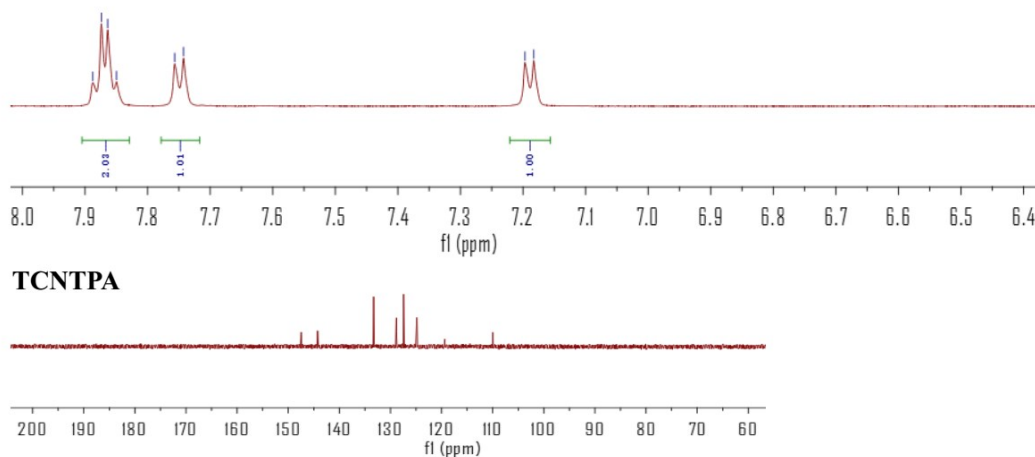
S2. Single molecular conductance measurement

The conductance experiments were conducted by using a home-built scanning tunneling microscopy (STM) break junction set-up[1-3] at room temperature. The Au tips were prepared by etching cleaned 0.2 mm diameter gold wires (99.99% pure) electrochemically, and cleaned by piranha solution, distilled water, and pure ethanol.

Pt tips were prepared by shearing the Pt wire (99.99% pure). Gold substrates were prepared by sequentially evaporating 5 nm Cr and 100 nm Au layers on silicon substrates with thermal evaporation. Pt substrates, bought from Top Vendor Science&Technology Co., Ltd., were prepared by sequentially evaporating 5 nm Cr and 150 nm Pt layers on silicon substrates with thermal evaporation. The Au and Pt substrates were cleaned with oxygen plasma for 10 minutes and hydrogen flame annealing for 1 min before each experiment. All experiments were measured in mesitylene (Sigma-Aldrich) with 1 mM target molecules. The initial approach of the gold tip in the z-axis is sequentially controlled by a stepper Picomotor (Newport, USA) and a piezo transducer (S-303.0L PI, Germany). During the conductance measurements, the tip movement is only controlled by the piezo. To achieve a high spatial resolution, the piezo is directly controlled by NI PXIe-4463 card. NI PXIe-4463 card is also used to generate the applied bias, and NI PXIe-4309 is used to record the current.

The STM-BJ experiments are controlled by a custom Labview program. The tip is repeatedly approached to and then retracted from the substrate at a constant bias (0.1 V, if not mentioned otherwise). For each cycle, the gold tip approaches to the gold substrate with PID (proportional-integral-derivative) control until the tip contacts the substrate to reach a conductance around 10 G_0. Then, the tip withdraws a distance of 20 nm at a speed of 20 nm/s. The typical total time for each cycle is about 2 s. The recorded G-D curves are analyzed by a custom labview program.

S3. Conductance measurements with Pt electrodes
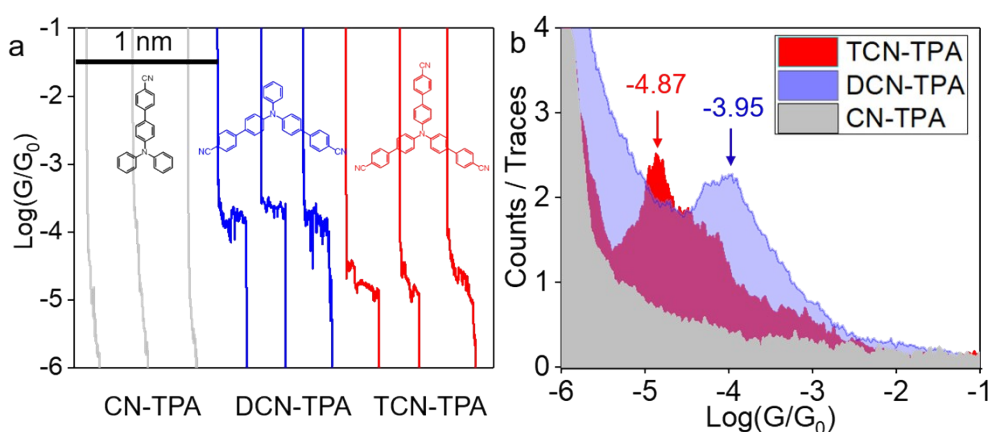
Figure S1 Sample conductance traces (a) and conductance histograms (b) for CN-TPA (grey), DCN-TPA (blue), and TCN-TPA (red) measured with Pt electrodes. All data were measured at 0.1 V bias, and the tip retraction speed is 20 nm/s.

The conductance histogram was obtained from 1000 conductance traces collected with Pt electrodes. The bin size was 50 bins/decade. In CN-TPA junctions (grey), no conductance step can be identified, and the corresponding histogram shows a smooth background. But for DCN-TPA (blue), and TCN-TPA (red) junction, the appearance of the conductance peaks indicates that a stable Pt-DCN-TPA-Pt or Pt-TCN-TPA-Pt molecular junction could be formed. Prominent peaks at $10^{-4.87}$ G_0 (red arrow) and $10^{-3.95}$ G_0 (blue arrow) can be generated from their statistical assessment of steps in their typical individual traces, respectively. The conductance trend on Pt substrate is consistent with the result obtained on the Au substrate. Their conductance (DCN-TPA and TCN-TPA) is also one order of magnitude differed. Given the very close work function between Au and Pt, and the resembled conductance trend obtained for three molecules, we expect that the same effect would be applicable to other metal substrates (such as Palladium) that addition of electron-withdrawing substituents to an electron-donating component would impact the metal-molecule electronic coupling and thus reduce the molecular conductance.

S4. 2D Conductance displacement histogram
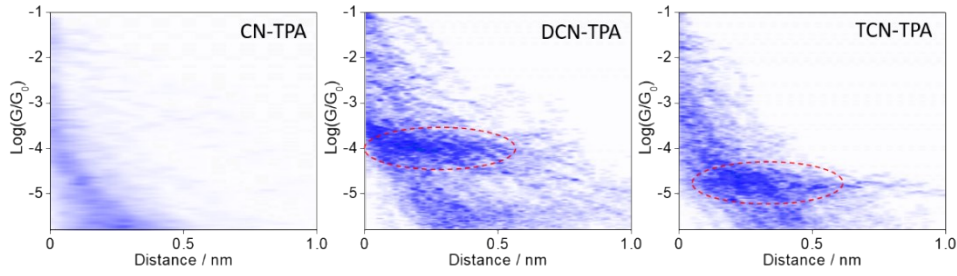
Figure S2. Conductance-displacement histogram for CN-TPA, DCN-TPA, and TCN-TPA. The dashed circles are indicative of the preferential conductance distributions.

Figure S2 show the 2D conductance-displacement histogram of CN-TPA, DCN-TPA, and TCN-TPA. The distance axis is linearly binned with 0.01 nm and the conductance axis is logarithmically binned with 50 bins each decade. All traces are aligned in a common distance scale by setting the first point with the conductance $G < 0.1 \ G_0$ to 0 nm. In Figure S1, it shows that there is no obvious signal for CN-TPA. But there is distinct conductance distribution for DCN-TPA around $10^{-3.9} \ G_0$ and TCN-TPA around $10^{-4.7} \ G_0$, which is in agreement with Figure 1. The distribution of the plateau lengths for DCN-TPA and TCN-TPA are all about 0.6 nm.

S5. Current-voltage measurements
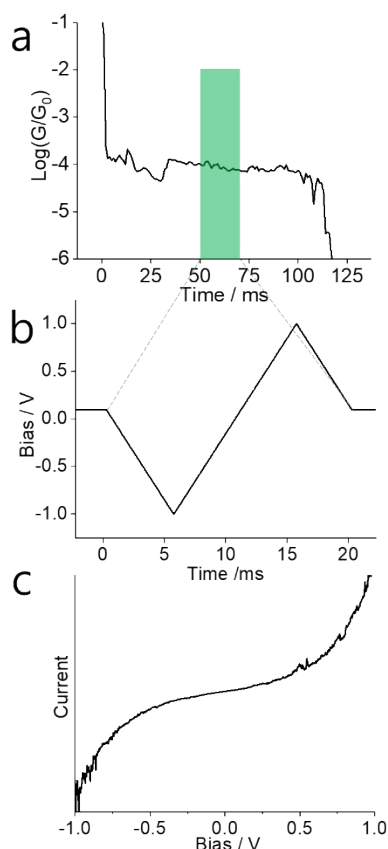
Figure S3. (a) Typical single molecule IV measurement showing a molecular plateau in the conductance decay. (b) A triangular voltage waveform applied. (c) The corresponding I-V curves.

Schematic illustration for conductance (current) change as a function of time in one cycle of the I-V measurement. After forming the metal contact, the Au tip was retracted at a bias voltage of 100 mV. Once a step was detected, the Au tip position was kept still for 20 ms. And a triangular voltage waveform was applied to avoid sudden voltage change that may cause chemical bond rupture[4]. After the voltage sweep, the tip was pulled further away from the substrate, then the whole process is repeated to generate a large number of IV traces for statistical analysis.
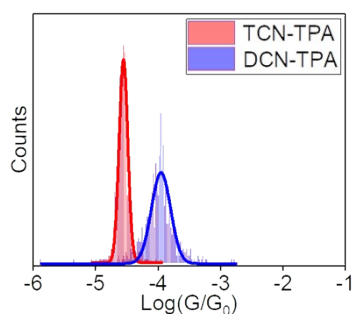
Figure S4. 1-D conductance histogram at 0.1 V for DCN-TPA (blue) and TCN-TPA (red) (dashed line in Figure 1d).

S6. Electronic structure and Transport calculations

Density functional theory (DFT) calculations were performed on the Gaussian 09_B01 package. The geometry of the ground state of the three molecules in the gas phase was optimized using B3LYP/6-31G (d, p) basic set. The surface charge of the N atom of CN moiety was acquired by showing the atomic charge number of the Mullikan type based on the optimized molecule structures. Correspondingly, they are -0.315, 0.313, and -0.311 for CN-TPA, DCN-TPA, and TCN-TPA, respectively.
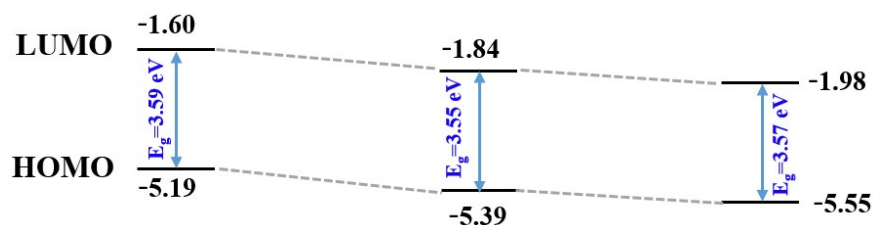
Figure S5. The calculated HOMO/LUMO of CN-TPA, DCN-TPA, and TCN-TPA.

Reference

1. Huang, M.; Sun, M.; Yu, X.; He, S.; Liu, S.; Nau, W. M.; Li, Y.; Wu, T.; Wang, Y.; Chang, S.; He, J., Reliably Probing the Conductance of a Molecule in a Cavity via van der Waals Contacts. *The Journal of Physical Chemistry C* **2020,** *124* (29), 16143-16148.
2. Yu, L.; Wang, Z.; Chen, H.; Guo, J.; Zhang, M.; Liu, Y.; He, J.; Chang, S., Long-Lived Gold Single-Atom Junctions Formed by a Flexible Probe for Scanning Tunneling Microscopy Applications. *ACS Applied Nano Materials* **2020,** *3* (4), 3410-3416.
3. Chen, H.; Li, Y.; Chang, S., Hybrid Molecular-Junction Mapping Technique for Simultaneous Measurements of Single-Molecule Electronic Conductance and Its Corresponding Binding Geometry in a Tunneling Junction. *Analytical Chemistry* **2020,** *92* (9), 6423-6429.
4. Xie, Z.; Ji, X.; Song, Y.; Wei, M.; Wang, C. J. C. P. L., More aromatic molecular junction has lower conductance. **2015,** *639*, 131-134.